BUILDING CHANGE DETECTION FROM DIGITAL SURFACE MODELS AND MULTI-SPECTRAL IMAGES

Franz Rottensteiner

Cooperative Research Centre for Spatial Information, Dept. of Geomatics, University of Melbourne,
723 Swanston Street, Melbourne VIC 3010, Australia - franzr@unimelb.edu.au

Commission III, WG III/4

KEY WORDS: Change Detection, Digital Surface Models, Data Fusion

ABSTRACT:

A new method for building change detection from Digital Surface Models (DSM) and multi-spectral images is presented. The DSM can be generated from Airborne Laserscanner (ALS) data or by image matching techniques. From the multi-spectral image, the Normalised Difference Vegetation Index (NDVI) is computed and used in the change detection process. The workflow of the method consists of two stages. In the first stage, the DSM, the NDVI, and surface roughness parameters derived from the DSM are used in a classification technique based on the Dempster-Shafer theory for data fusion. In the case of ALS data, the height differences between DSMs created from first and last pulse data can also be considered. This technique is used to detect buildings. In the second stage of processing, these building detection results are compared to an existing building data base, and changes between the existing data base and the new data set are determined. This paper focuses on the second processing stage, in which the actual change detection is carried out. The method is designed to classify buildings and building parts as being *confirmed*, *changed*, *new*, or *demolished*. The change detection method considers the facts that the original data and the building detection results can have a different topology and that small differences between the data from the two epochs might be caused by different levels of generalisation or errors caused by a misalignment or insufficient resolution of the sensor data. Examples for the performance are given using DSMs generated both from ALS data and by image matching, highlighting the different properties of these data for building change detection.

1. INTRODUCTION

1.1 Motivation and Goals

Automatic building detection has been an important topic of research in Photogrammetry for more than a decade. In order to achieve results compliant with mapping scales of 1:1000-1:10000, multi-spectral aerial imagery and/or airborne laser scanner (ALS) data have been used (Matikainen et al., 2003; Rottensteiner et al., 2007). In many industrialised countries there exist 2D maps or building databases. Due to the dynamic nature of industrialised societies, building data collected at a certain time become outdated rather quickly. To speed up the production cycle for keeping such databases up-to-date, it is desirable to automate the detection of areas where buildings have changed. It is the goal of this paper to describe such a method for building change detection based on Digital Surface Models (DSMs) and multi-spectral imagery. This method is based on an adaptation of previous work on automatic building detection (Rottensteiner et al., 2007). The building detection results are compared to the existing map, and a classification is carried out to determine the changes between the two epochs. This classification has to take into account deviations between the two data sets that might be due to different degrees of generalisation and to small registration errors between the original data captured at the two epochs. It also has to consider the fact that the topology of the existing map and the automatically detected buildings might be different (Ragia and Winter, 2000). The method will be applied to DSMs generated from ALS data and by digital image matching, showing how well these different data sets are suited for the purpose of change detection for updating existing building data bases.

1.2 Related Work

There are two basic approaches to the problem of change detection (Vosselman et al., 2004). If original data are available for two different epochs t_1 and t_2, change detection can be carried out by comparing the two datasets and inferring changes from the differences detected in the original data. This has been applied in the past to detect changes in buildings after earthquakes based on their different appearance in DSMs generated by ALS (Murakami et al., 1998). In the second scenario, a map or a digital data base is available for epoch t_1 and original data are only available for epoch t_2. Change detection is carried out to keep the map up-to-date. In order to infer changes, the original map can be compared to the new sensor data directly. If ALS data are used for change detection, changes in buildings will result in height differences between a 3D city model and the new DSM. However, if the original data are only available in 2D, this cannot be directly exploited. This problem can be circumvented by detecting the objects of interest independently in the new sensor data and comparing the object detection results to the original map (Vosselman et al., 2004). This strategy does not take into consideration the fact that a building exists in the original map, it is not unlikely that there will still be a building at epoch t_2.

Matikainen et al. (2003, 2004) detect buildings in ALS and aerial image data and then compare the results to building segments from an existing map. The method applies rule-based classification techniques separately to the building detection results and to the buildings of the existing map, based on the percentage of the area of a building that overlaps with any building in the other data set. Buildings in the existing data set are classified as *detected*, *partly detected*, and *not detected*,

whereas buildings in the new data set are classified as *new*, *enlarged*, or *old*. Small errors caused by alignment errors and by the generalisation of the existing map are considered by selecting thresholds different from 100% for classifying a building as *old* or *detected*. A common visualisation of these two classification results is presented on a per-pixel basis, but no further object-based analysis is carried out.

Vögtle and Steinle (2004) present a method for building change detection from ALS data that is based on a comparison of an existing map and the DSM corresponding to that map with the newly detected buildings and the corresponding DSM. Change detection results in a classification of buildings as *not-altered*, *new*, *demolished*, *added-on*, or *reduced*. In a first step, the overlap ratio between buildings is evaluated for both the old and the new data set. This leads to an initial classification of buildings as *new*, *demolished*, or *other*. The buildings not yet classified have a correspondence in the other data set, and are further classified as *not-altered*, *added-on*, or *reduced* based on an analysis of the height changes of the DSM in the areas covered by corresponding segments. Thus, this is an example for a change detection algorithm that uses the original data for both epochs. The advantage that this method can also detect height changes is contrasted by the problem of actually having access to such data.

Vosselman et al. (2004) present a method for comparing an existing map with the results of a building detection technique using ALS data. They give a list of errors that might result in differences between the existing map and the newly extracted buildings, namely generalization, random noise, systematic alignment errors, and object selection, the latter being a variety of generalization. Morphologic filters are applied before the comparison of the two data sets to compensate for errors caused by generalization, and an offset between corresponding segments is determined by a matching technique for coping with alignment errors.

In (Rottensteiner et al., 2007), a method for building detection by the fusion of ALS data and a normalised difference vegetation index (NDVI) derived from the red and the infrared bands of a multi-spectral image was presented. This method has been modified so that it can be applied to building change detection. The main focus of this paper will be on describing a new change detection method that is based on a comparison of the existing map and the results of building detection.

1.3 Method Overview

Building change detection requires a DSM generated either from ALS data or by image matching and, optionally, an NDVI image generated from a geocoded multi-spectral image. The DSM, the NDVI, and surface roughness parameters derived from the DSM are used in a building detection technique based on the Dempster-Shafer theory for data fusion. In the case of ALS data, the height differences between DSMs created from first and last pulse data can also be used. This classification technique has been modified so that it can also consider the existing building data base. An outline of the modified building detection method will be given in Section 2. In a second processing stage, the results of building detection are compared to an existing building data base and changes between the existing data base and the new data set are determined. This method can handle data sets of different topology and will be described in Section 3. Section 4 will present first results, whereas conclusions will be drawn in Section 5.

2. BUILDING DETECTON

The input to the method for building detection presented in (Rottensteiner et al., 2007) comprises up to four data sets generated from the raw data in a pre-processing stage. The minimum set of input data consists of a DSM grid and a Digital Terrain Model (DTM). The DSM can be derived from ALS data or by image matching. For the experiments described in Section 4, the DTM was derived from the DSM by hierarchic morphologic filtering (Rottensteiner et al., 2005). If ALS data are used, a DSM grid representing the height differences between the first and the last pulse can also be used. The fourth data set that can be used in building detection is the NDVI.

Building detection is based on the theory of Dempster-Shafer for data fusion. In Dempster-Shafer fusion, the output of a set of "sensors" is used for a classification process in which n classes $C_j \in \theta$ are to be discerned. Denoting the power set of θ by 2^θ, a *probability mass* fulfilling certain constraints has to be assigned to every class $A \in 2^\theta$ (i.e., also to any combination of the original classes) by each sensor. The probability masses from the individual sensors can be combined, and from these combined probability masses, two parameters can be computed for each class: the *Support* of a class is the sum of all masses assigned to that class, and the *Plausibility* sums up all probability masses not assigned to the complementary class of A. The accepted hypothesis $C_a \in \theta$ is determined according to a decision rule. The Dempster-Shafer theory also provides a measure for the *Conflict* in the sensor data (Klein, 1999).

Building detection starts with a Dempster-Shafer fusion process carried out for each pixel of the DSM to achieve a classification of the input data into one of four classes: buildings *(B)*, trees *(T)*, grass land *(G)*, and bare soil *(S)*, thus $\theta = \{B, T, G, S\}$. The model for the distribution of the evidence from each sensor to the four classes assumes that each sensor i can separate two complementary subsets of θ, U_{Ci} and U_{Ci}'. The probability mass $P_i(x_i)$ assigned to U_{Ci} by the sensor i depending on the sensor output x_i is modelled to be equal to a constant P_l for $x_i < x_l$. For $x_i > x_u$, it is modelled to be equal to another constant P_u, with $0 \le P_l < P_u \le 1$. Between x_l and x_u, the probability mass is modelled by a cubic parabola with horizontal tangents at $x_i = x_l$ and $x_i = x_u$. The probability mass $[1 - P_i(x_i)]$ is assigned to U_{Ci}'. No other assumptions about the distributions of the sensor data with respect to the classes are required. The combined probability masses are evaluated for each pixel, and the pixel is assigned to the class of maximum support. Originally, up to five "sensors" could be used in this process. The height differences ΔH between the DSM and the DTM help to distinguish elevated objects from the ground, thus $U_{C\Delta H} = B \cup T$. Two surface roughness parameters computed from the first derivatives of the DSM, namely strength R and directedness D, are also used in the classification process. Large values of surface roughness are typical for trees, thus $U_{CR} = T$ and $U_{CD} = T$. However, D is only used if R differs significantly from 0. The height differences ΔH_{FL} between the first and the last pulse DSMs also distinguish trees from other classes: $U_{C\Delta HFL} = T$. Finally, the NDVI is an indicator for vegetation, thus $U_{CNDVI} = T \cup G$. The uncertainty of the NDVI in shadow areas can be considered by modulating the probability masses depending on the standard deviation of the NDVI. In (Rottensteiner et al., 2007) it was shown how the parameters of the model for the probability masses can be selected. The classification results are improved by a post-classification technique aiming at re-classifying isolated pixels and pixels having a high conflict value. Initial building regions

are determined as connected components of "building pixels". A second Dempster-Shafer fusion process is applied to these regions, using four cues representing average values for each building region to eliminate regions actually corresponding to trees. The result of building detection is the label image of the remaining building regions. The boundaries of these building regions can be extracted in vector format, too.

For the purpose of building change detection, a further optional input "sensor" was integrated into the first Dempster-Shafer fusion process. In many scenes, the amount of change will not be high, so that the original map gives an indication where buildings are to be expected. Thus, if a pixel is situated inside a building in the original map, it is more likely still to be inside a building at epoch t_2 than not. On the other hand, if the pixel is not inside a building in the original map, it is also more likely that it is not inside a building at epoch t_2. Let the probability that a pixel inside a building in the original map is still a part of a building at epoch t_2 be denoted by P_B, and the probability that a pixel not being inside a building in the original map is not inside a building at epoch t_2 by $P_{\neg B}$. For a pixel inside a building in the original map, a probability mass equal to P_B can be assigned to class B, and $(1 - P_B)$ to class $T \cup G \cup S$. If the building is not inside a building in the original map, $P_{\neg B}$ is assigned to class $T \cup G \cup S$ and $(1 - P_{\neg B})$ is assigned to class B. Thus, a bias is introduced by the original map, which can especially help to confirm small buildings that might otherwise be classified as trees. In the current implementation, $P_{\neg B} = P_B$ is assumed, and the user has to specify the value for P_B. Typically, P_B is chosen between 60 % and 75 %. The user can also decide not to consider the original map in the classification if the amount of change in the scene is high.

3. BUILDING CHANGE DETECTION

Change detection is based on a comparison of label images: the "existing label image" generated from the existing map and containing the labels $l^e \in L^e$, and the "new label image" generated by the building detection method and containing the labels $l^n \in L^n$. The goal of change detection is three-fold:

1. A classification of the buildings in the existing map as either *confirmed*, *changed*, or *demolished*;
2. The detection of buildings that are found to be *new*;
3. A delineation of the outlines of both the *changed* and the *new* buildings, showing *demolished* and *new* building parts for the *changed* buildings.

Since the two data sets will usually have different topologies, these goals are achieved in a procedure consisting of two stages. The first stage is a topological clarification of the new data set by matching its labels to those of the existing label image in order to achieve topological consistency between the two epochs. This is followed by the actual classification to detect the changes. The output of change detection consists of a "change map" showing the actual changes between the epochs according to the classification results described above, and a label image describing the state at epoch t_2.

3.1 Topological Clarification

For each co-occurrence of two labels $l^e \in L^e$ and $l^n \in L^n$, the overlap ratios $p_{ne} = n_{n \cap e} / n_n$ and $p_{en} = n_{n \cap e} / n_e$ are computed, where $n_{n \cap e}$ is the number of common pixels assigned to the

region l^n in the new label image and to l^e in the existing label image, n_n is the total number of pixels assigned to the region l^n in the new label image, and n_e is the total number of pixels assigned to l^e in the existing label image. First, marginal correspondences, i.e. correspondences that do neither contribute significantly to l^n nor to l^e, are eliminated. Using a user-defined threshold t_m (typically, 10 %), all correspondences with $p_{ne} < t_m$ and $p_{en} < t_m$ are eliminated. As a result, a set of correspondences between labels $l^e \in L^e$ and $l^n \in L^n$ is obtained. Figure 1 shows two sets of labels L^e and L^n, with correspondences depicted by lines. If the topology of the two data sets were identical except for *new* or *demolished* buildings, each label would have no or one line connecting it to a label in the other data set. As the topology is not identical, six cases must be distinguished (cf. Figure 1):
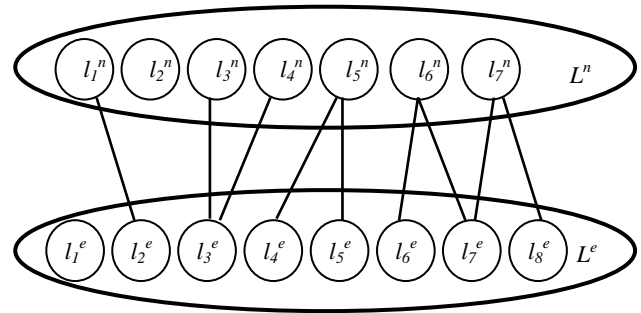

Figure 1. Two sets of labels L^e and L^n and correspondences between labels $l_i^e \in L^e$ and $l_j^n \in L^n$.

1. A label in L^e not having any corresponding label in L^n indicates a *demolished* building (e.g. l_1^e in Figure 1).
2. A label in L^n not having any corresponding label in L^e indicates a *new* building (e.g. l_2^n).
3. A label in L^e having exactly one corresponding label in L^n (e.g. l_2^e and l_1^n) indicates a *confirmed* or a *changed* building.
4. If a label in L^e has M corresponding labels in L^n (e.g. l_3^e, l_3^n and l_4^n), the original building is split into several labels. It can be either *confirmed* or *changed*. The splitting can be caused by the actual demolition of building parts, or it can just be caused by height discontinuities within a building.
5. If a label in L^n has N corresponding labels in L^e (e.g. l_5^n, l_4^e and l_5^e), several existing buildings are merged. Again, this might be the result of some actual changes or not. It typically occurs with terraced houses having identical roof heights.
6. If a set of M labels $l_i^e \in L^e$ corresponds to a set of N labels $l_j^n \in L^n$ (e.g. l_6^e, l_7^e, l_8^e, l_6^n and l_7^n), buildings or building parts are both split and merged, and there are ambiguities with respect to the correct correspondence of some of the new labels (Figure 2).

In all except the first two cases, there can additionally be building parts that overlap with the background in the other label image, i.e., *new* or *demolished parts* of *changed* buildings.

In order to obtain a classification on a per-building level for all existing buildings, the ambiguous case 6 has to be resolved first. Assuming the topology of the existing label image to be correct, the new label image has to be changed so that no ambiguities occur. This can be achieved by splitting any label l_j^n that corresponds to more than one label in L^e and / or has a significant overlap with the background. This shall be explained using the example in Figure 2. The existing label image, shown in the upper row, contains two labels l_1^e and l_2^e. The second row shows the results of building detection. There are altogether five

labels l_j^n, one of which (l_2^n) overlaps with both l_1^e and l_2^e. The label l_4^n also contains a new building that has been constructed in a gap within the building l_2^e. First, new buildings or building parts are identified. For this purpose, a binary image of those building pixels in the new label image that correspond to the background in the existing label image is generated. This binary image highlights the *new* building pixels, but it is also affected by noise at the building outlines. A morphological opening filter is used to remove the noise. The size of the structural element is the minimum size of a change that can be detected, and is typically chosen to correspond to one to three times the sensor resolution. If there remain "white" pixels in the filtered image, new labels corresponding to new building parts can be detected by a connected component analysis. A label image L^c combining the existing labels L^e and these new labels is created. Each label in L^n corresponding to more than one label in L^c is split so that each of the new labels corresponds to exactly one label of L^c. In order to compensate for smoothing effects of the morphological filter at the fringes of new building parts, the Voronoi diagram of L^c is used to assign pixels to one of the new labels. The third line of Figure 2 shows the results of this splitting process. Two new labels were added to L^n. The label l_6^n corresponds to a new building part, and the label l_7^n is the result of splitting off the part of l_2^n that corresponds to l_2^e.
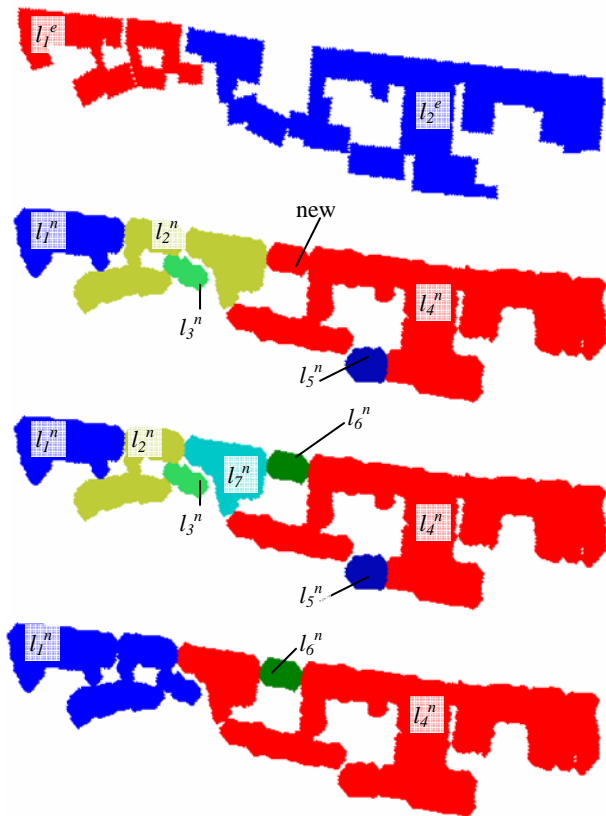

Figure 2. First row: Existing map. Second row: Results of automatic building detection. Third row: New label image after resolving ambiguities. Fourth row: Results of topological clarification.

Having resolved all ambiguities, the case corresponding to merged labels is resolved. Labels can be merged because the buildings are close to each other (left part of Figure 3), or because a new building has been constructed between them (right part of Figure 3). In a similar process as described above, new building labels are detected, and the merged label in L^n is

split into several new labels, each corresponding either to a new building or to exactly one label in the existing map.
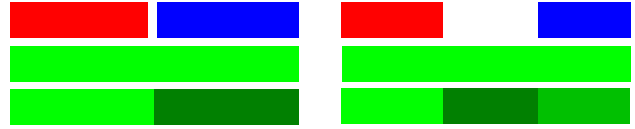

Figure 3. Clarifying the case of merged labels. Upper row: Existing map with two buildings. Second row: Results of building detection. Third row: Clarified label image. Left: the merged buildings are close to each other. Right: a new building was detected.

Finally, the case corresponding to split labels is analysed. We want to merge all new labels corresponding to an existing label if the fact that these labels are separate in the new label image is not the result of a larger building part having been demolished. For that purpose, the new labels are grown by morphologic closing (i.e., the binary image of building pixels is closed morphologically, and each building pixel in the closed image is assigned to the label found in the Voronoi diagram of the new label image). If two labels are found to be neighbours in the closed label image, the two labels are merged. If this is not the case, the separation is assumed to have been caused by the demolition of a building part, and the original labels are maintained. The last row in Figure 2 shows the results of topological clarification after merging of the split labels. As a result of topological clarification, an improved version L^n_{imp} of the new building label image L^n is obtained, with some of the original labels in L^n having been split and others having been merged. Each of the labels in L^n_{imp} corresponds either to exactly one label in L^e or to none (Figure 4). Each of the labels of L^e corresponds to one or more labels of the improved version of L^n_{imp} or to none. There remaining split cases (one label of L^e corresponding to more than one label in the improved version of L^n_{imp}) all correspond to *changed* buildings.
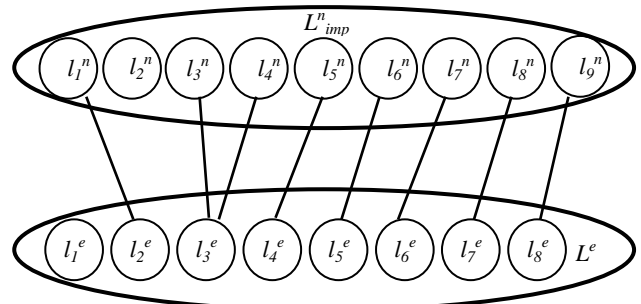

Figure 4. Two sets of labels L^e and L^n_{imp} and correspondences between labels $l_i^e \in L^e$ and $l_j^n \in L^n_{imp}$ after topological clarification.

3.2 Classification of Changes

After topological clarification, the actual change detection is carried out. Again, the percentages of overlap are computed for each co-occurrence of two labels $l^e \in L^e$ and $l^n \in L^n_{imp}$. Marginal correspondences are eliminated, which results in a correspondence graph like the one shown in Figure 4. A building is classified as *new* if its label $l^n \in L^n_{imp}$ does not have a correspondence in L^e. An existing building is classified as *demolished* if its label $l^e \in L^e$ does not have a correspondence in L^n_{imp}. For all remaining building labels $l^e \in L^e$, two binary images are created: a binary image of *demolished* pixels (i.e., pixels assigned to l^e in the existing map, but not to any of the

corresponding labels in L^n_{imp}), and a binary image of *new* pixels (i.e., pixels assigned to any of the labels corresponding to l^e in L^n_{imp}, but not assigned to l^e in the existing map). Both are filtered by morphological opening. The size of the structural element is chosen to be identical to the one used in topological clarification. If neither *demolished* nor *new* pixels remain after morphological opening, the existing building is classified as *confirmed*; otherwise, it is classified as *changed*. For *changed* buildings, connected components in the binary images of *demolished* and *new* pixels are considered to correspond to *demolished building parts* and *new building parts*. Finally, two images representing the change detection results are generated:

1. A *change map* using different colours for *new*, *demolished*, *confirmed*, buildings as well as for *confirmed*, *new*, or *demolished parts* of *changed* buildings.
2. A label image representing the new state.

For generating the label image representing the new state, there are two options. The first option is to use the improved version of the new label image. As an alternative, the original building outlines can be used for *confirmed* buildings, whereas for *changed* buildings, the outlines can be a combination of the original outlines for those building parts that have not been changed and the *new building parts*. The second option is to be preferred if the original map is more accurate, e.g. if it is a cadastral map generated by a geodetic survey.

4. EXPERIMENTS

The method described in this paper was tested using two data sets. The first data set, captured over Fairfield (NSW), consisted of ALS points with a nominal spacing of 1.2 m. The first and the last laser pulses as well as the intensity of the returned signal were recorded. In addition, a colour orthophoto was available. From the red band of that orthophoto and the intensity of the signal, a "pseudo-NDVI" image could be generated. DSMs of a grid width $\Delta = 1$ m were generated for both the first and the last pulse data. For a part of the Fairfield data set, the outlines of the buildings were determined by photogrammetric plotting with a planimetric accuracy of ±0.2 m. In order to simulate actual changes, the label image generated from these outlines was modified by both adding and removing buildings or building parts. This modified building map was used as the existing map in change detection. The size of the test area was about 500 x 400 m^2. The second data set was provided by EuroSDR. It consisted of a DSM generated by image matching, a colour orthophoto and an orthophoto representing the infrared band, and an existing building data base in the form of a binary building image. Both the DSM and the orthophoto had a resolution of $\Delta = 0.501$ m. The size of the test area was about 1100 x 1100 m^2. The DSM was very noisy, especially in the shadow regions, where the outlines of buildings were smoothed. The numerical resolution of the DSM heights was identical to the planimetric resolution Δ. Thus, the only height values occurring were full multiples of Δ. Along with the uncertainties of the DSM in shadow areas, this was the reason why surface roughness was of no use for building detection.

Building detection using the method outlined in Section 2 was applied to both data sets. In Fairfield, standard parameters described in (Rottensteiner et al., 2007) were used for the height differences between DSM and DTM, the height differences between first and last pulse DSMs, the NDVI, and the two

surface roughness parameters. The existing map was also considered in the classification process, using $P_B = P_{\neg B} = 75$ %. In Toulouse, we used the DSM, the NDVI, the directedness of surface roughness (but not the strength), and the existing map, using $P_B = P_{\neg B} = 60$ % and selecting the other parameters in the way described in (Rottensteiner et al., 2007). As described in Section 3, the results of building detection were used to detect changes between the original map and the new data. The resulting change maps, generated at the resolution of the respective DSM grids, are presented in Figure 5.

Figure 5. Change maps for Fairfield (above) and Toulouse below). Ochre/yellow: *confirmed* buildings/building parts. Blue/light grey: *demolished* buildings/building parts. Red/green: *new* buildings/building parts.

In Fairfield, changes affecting the main buildings are detected correctly. All *new* buildings (red areas in Figure 5) and building parts (green) in the data set were detected. All *new* buildings are correct, and so are the majority of the *new* building parts. The few incorrect *new* building parts are the result of an over-estimation of the building extents. Of course, the algorithm cannot really discern whether a larger area found to be new is a new building or only a new building part. In case of doubt, a new building is assumed. All *demolished* buildings (blue) and building parts (light grey) were detected. All except two *demolished* building parts are correct. However, with *demolished* buildings, the trend observed in (Rottensteiner et

149

al., 2007) is confirmed: For the main buildings, the change detection results are correct, but for smaller structures, the results become more and more uncertain. Thus, the small buildings classified as *demolished* in the back yards, mostly garden sheds and garages, are actually too small to be detected by the method and hence have to be considered as false negatives. A comparison of the label image representing the new state to the reference label image was carried out to derive quality parameters on a per-pixel level. *Completeness*, *correctness*, and *quality* (Rottensteiner et al., 2005) were determined for the building pixels of the label image representing the new state. *Completeness* was 95.0 %, thus 5 % of the building pixels in the reference data set were not detected; these are mostly small buildings in the back yards. *Correctness* was 97.9 %, thus only 2.1 % of the detected building pixels were incorrect. The overall *quality* was 93.1 %. These numbers represent the actual classification accuracy and are not affected by misalignment of the data sets, because the original outlines were used for *confirmed* buildings.

In Toulouse, the results are not as good as for Fairfield. Again, it can be observed that small buildings are not detected in the new data set. Many major changes are detected correctly, e.g. the groups of *new* and *demolished* buildings in the south-west of the scene. There are two very large areas of false detections: the large green area in the northeast corner of the scene merges a correctly detected new building with a parking lot, and the large red area in the east is actually a sports field. In both cases, as well as in the case of some building parts erroneously classified as *demolished*, the poor quality of the DSM in these areas (height variations larger than 3 m in essentially horizontal areas) contributed to these false classifications. Note also the obvious over-estimation of the large building complex in the western part of the scene in the shadow areas (i.e., north of the building). Other problems were related to trees partly overhanging buildings and to the general lack of ground points in the forested areas, the latter causing errors in the DTM generation process. On a per-pixel basis, *completeness* was determined to be only 89.3 %, and *correctness* was even poorer (68.1 %). Without the two problematic areas, *correctness* was still only 76.5 %. These data are partly afflicted by errors in the reference data. They were determined by digitization in the orthophoto and, thus, are not as accurate as the Fairfield reference data. In any case, a comparison of the results for the two data sets shows the importance of using a high-quality DSM in the classification process.

5. CONCLUSIONS

A new method for building change detection was presented. It combines DSMs, DSM roughness parameters, an NDVI image, and an existing map in a classification process based on Dempster-Shafer fusion. Comparing the building detection results to the existing map, a topological clarification is carried out, and the changes between the existing map and the results of building detection are classified. The classification takes into account the fact that small differences are likely to be caused by errors of building detection at the building outlines. The results of change detection are presented so that the user can easily assess which buildings are *confirmed*, *new*, *demolished*, or *changed*, and in case of *changed* buildings also the nature and extent of these changes. Given the importance of the DSM in the classification process, it is not astonishing that the method works considerably better with DSMs derived from ALS data compared to DSMs generated by image matching. However,

this may be partly the result of the specific matching algorithm used to generate the Toulouse DSM. In the future, the method will be tested further using the remaining EuroSDR data sets. Further work will concentrate on improving the geometrical quality of the building outlines by image edges, because the building outlines are much better defined in the image data than in a DSM, especially if the latter was generated by matching.

REFERENCES

Klein, L., 1999. *Sensor and data fusion, Concepts and applications*. 2nd edition, SPIE Optical Engineering Press.

Matikainen, L., Hyyppä, J., Hyyppä, H., 2003. Automatic detection of buildings from laser scanner data for map updating. In: *The International Archives of the Photogrammetry, Remote Sensing and Spatial Information Sciences*, Dresden, Germany, Vol. XXXIV, Part 3/W13, pp. 218-224.

Matikainen, L., Hyyppä, J., Kaartinen, H., 2004. Automatic detection of changes from laser scanner and aerial image data for updating building maps. In: *The International Archives of the Photogrammetry, Remote Sensing and Spatial Information Sciences*, Istanbul, Turkey, Vol. XXXV, Part B2, pp. 434-439.

Murakami, H., Nagakawa, K., Shibata, T., Iwanami, E., 1998. Potential of an airborne laserscanner system for change detection of urban features and orthoimage development. In: *The International Archives of the Photogrammetry and Remote Sensing*, Stuttgart, Germany, Vol. XXXII, Part 4, pp. 422-427.

Ragia, L., Winter, S., 2000. Contributions to a quality description of areal objects in spatial data sets. *ISPRS Journal for Photogrammetry and Remote Sensing* 55 (3), pp. 201–213.

Rottensteiner, F., Trinder, J., Clode, S., Kubik, K., 2005. Using the Dempster Shafer method for the fusion of LIDAR data and multi-spectral images for building detection. *Information Fusion* 6 (4), pp. 283-300.

Rottensteiner, F., Trinder, J., Clode, S., Kubik, K., 2007. Building detection by fusion of airborne laserscanner data and multi-spectral images: Performance evaluation and sensitivity analysis. *ISPRS Journal for Photogrammetry and Remote Sensing*, 62(2), pp. 135–149.

Vögtle, T., Steinle, E., 2004. Detection and recognition of changes in building geometry derived from multitemporal laserscanning data. In: *The International Archives of the Photogrammetry, Remote Sensing and Spatial Information Sciences*, Istanbul, Turkey, Vol. XXXV, Part B2, pp. 428-433.

Vosselman, G., Gorte, B., Sithole, G., 2004. Change detection for updating medium scale maps using laser altimetry. In: *The International Archives of the Photogrammetry, Remote Sensing and Spatial Information Sciences*, Istanbul, Turkey, Vol. XXXV, Part B3, pp. 207-212.